UCRL-5636
Health and Safety-UC-4 1
TID-4500 (15th Ed.)

UNIVERSITY OF CALIFORNIA
Lawrence Radiation Laboratory
Livermore, California

Contract No. W-7405-eng-48

MEASUREMENT OF RADIOACTIVE FALLOUT AIR SEDIMENTATION APPARATUS

John F. Lakner

July 1959

Printed for the U.S. Atomic Energy Commission

DISCLAIMER

Printed in USA. Price $1.00. Available from the
Office of Technical Services
U. S. Department of Commerce
Washington 25, D.C.

MEASUREMENT OF RADIOACTIVE FALLOUT AIR SEDIMENTATION APPARATUS

John F. Lakner

Lawrence Radiation Laboratory, University of California
Livermore, California

ABSTRACT

An apparatus involving a fundamental idea of air sedimentation has been adapted to fractionate radiological fallout samples (size range $D\rho^{0.5} = 2$ to $D\rho^{0.5} = 240$) and measure their radioactivity. This paper describes the principle involved, its limitations, and many of the characteristics of the apparatus. A discussion is included on the use of probability paper for size distribution analysis.

MEASUREMENT OF RADIOACTIVE FALLOUT AIR SEDIMENTATION APPARATUS

CONTENTS

INTRODUCTION

Purpose

An apparatus was required to measure the radioactive distribution of particles from a cloud formed by a nuclear detonation. By knowing how the radioactivity distributes itself among the various particle sizes, one could determine whether major radiological fallout occurred in the blast vicinity or was disseminated elsewhere. Furthermore, an analysis of each fraction permitted the determination of a distribution for the radioactive elements in the original sample.

Requirements of the Problem

In order to obtain a radioactivity distribution vs particle size distribution, some method of first fractionating the fallout samples and then counting the activity was needed. The problem was made difficult for several reasons: (1) Because subsequent samples were not to be contaminated, decontamination of the equipment needed to be thorough. (2) A large number of samples meant that the apparatus should be able to produce results in a short time. (3) The apparatus would have to handle samples less than 1 gram. (4) The method was best that closely approached that of the actual fallout conditions. (5) Liquid sedimentation was out of the question due to possible effects of solvent on the sample.

Of all the methods mentioned in the literature,[1,2,3] it was felt that taking cuts from a column of particles falling in air and counting each cut after it was removed from the collection mechanism provided the best solution. The theoretical basis of the method was available in Stokes' Law.

Scope of the Work

Previous developments[4,5] have used the radioactivity of particles to measure the particle size distribution in powders. The methods were based on the assumption that the powders were homogeneous and that radioactivity was proportional to the mass of the particles.* Although this

*The activity that radiates from a thin lamina of suspension is used as a measure of the weight of material in the lamina. During irradiation the activity generated in a particle is proportional to the number of atoms in the particle. Consequently, the relative activity between two particles will be equal to their relative weights.

past work was of general interest, the method described was not directly adaptable to our purpose.

A Micromerograph (Sharples Corp.) was already available. With this instrument as a starting point, the design and fabrication of a fractionating mechanism and the installation of a counter* were undertaken. The characteristics of this new apparatus, hereinafter called a "Micromero-multipan", are described in this report.

Most of the data has been obtained with powdered coral. The remainder of the data has been obtained by using as many fallout samples as were available for this purpose.

It was not felt necessary in this report to render a discussion of the actual radioactivity counting procedure.

THEORETICAL BACKGROUND

The determination of a size frequency** relationship for a powder necessitates the determination of the weight of material falling within a number of size groups; each of which groups cover a known small range of particle sizes. In most types of test for the size frequency analysis of material in the sub-sieve*** range, the sizing is carried out by methods based on the motion of particles relative to a viscous fluid, that is, either sedimentation[6] or elutriation.

The most commonly used procedure for the analysis by the sedimentation method is that in which the powder is initially dispersed into a stationary column of fluid at the beginning of the test. At any later time there will be a density gradient along the column due to particles falling through the fluid under the influence of gravity.

---

*This counter was to be used only for "roughing." Proper shielding was necessary for counting to be done directly on the apparatus in order to eliminate the influence of adjacent fractions or size groupings.

**On occasions $D\rho^{0.5}$ or fall rate is used. $D\rho^{0.5}$ is useful where ρ (density) is not available.

***This is considered to be < 200 mesh (74μ) although sieves to 400 mesh are available.

If now a cut is withdrawn from the bottom of the column at a definite time, t, after the commencement of the run, then the smallest particle in this sample will be that which had fallen from the cloud suspension in time, t. The next sample withdrawn from the bottom of the column will have all those particles which had fallen in the following time interval, Δt_1. The third cut will have material which had fallen in the time interval Δt_2, etc.

If now the residue on each pan is weighed, a cumulative percent by weight smaller (or larger) than a given particle size curve may be built up and this curve then provides a size frequency distribution of the sample.

The smallest particle on the first pan will have a terminal velocity equal to H/t, H being fall distance. From Stokes' Law, equations (1) and (2), the diameter or $D_\rho{}^{0.5}$ can be calculated. Figure 1 shows $D_\rho{}^{0.5}$ plotted versus time. This curve* represents the corrected form of Stokes' Law which takes into account the deviations from the Stokes' Law drag force and the initial distance the particles travel (deceleration distance) before attaining their terminal velocities.

$$v_t = \frac{10^{-8} \rho g D^2}{\mu} \tag{1}$$

or

$$D_\mu = \sqrt{\frac{18 \mu H}{10^{-8} t g (\rho_1 \rho_2)}} \tag{2}$$

where

v_t = terminal velocity at time, t.

D_μ = diameter in μ ($1\mu = 10^{-4}$ cm) of a sphere having the same rate of fall in a viscous fluid under streamline conditions.

μ = viscosity of the fluid (1.82×10^{-4} poises for air at 20°C)

g = constant of gravitation (980 dynes/cm^2).

ρ_1 = density of the particle (g/cc)

ρ_2 = density of fluid (g/cc)

t = time (sec)

H = fall distance (cm).

*Runs were made using spherical powders of varying density and size and having known narrow size distributions.

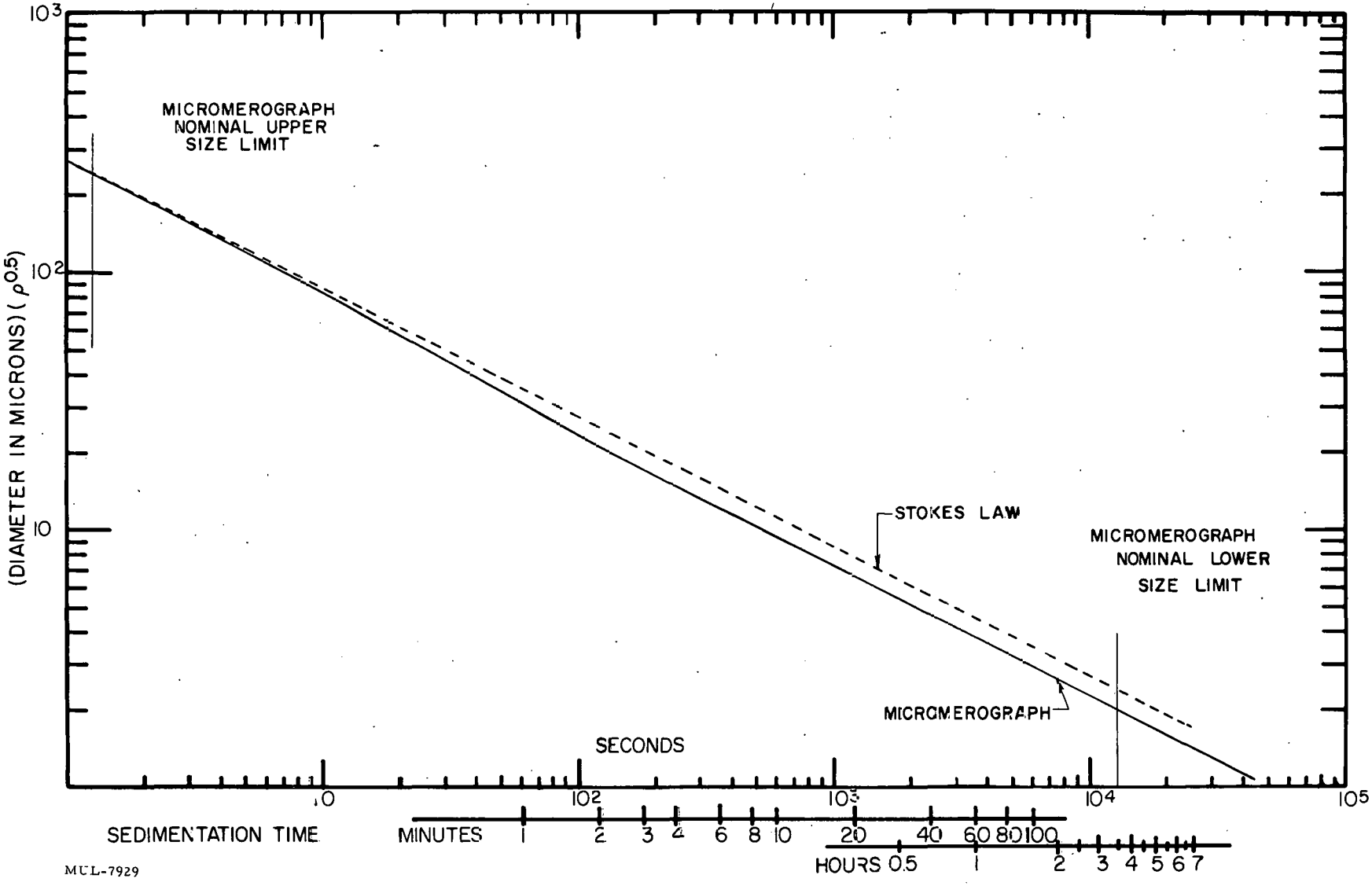

Fig. 1. Plot of $D\rho^{0.5}$ versus settling time.

The conditions established for the validity of Stokes' Law are:

(1) The motion of the particle in the fluid is laminar.

(2) The fluid extends for an infinite distance in all directions around the particles.

(3) The mean free path of the molecules is small compared with the diameter of the particle.

For small particles moving in a gas at low pressure, an error is introduced by neglecting the last item. An approximate correction to the velocity of fall is given by Rose[7]:

$$v_t = v_\rho \left(1 + 1.8 \frac{\lambda}{d}\right)$$

where v_ρ = the velocity calculated from Stokes' Law.

λ = mean free path of the molecules.

v_t = corrected velocity of fall.

d = particle diameter.

APPARATUS AND PROCEDURE

Apparatus

Figures 2 and 3 illustrate the apparatus which was finally developed. The major segments portions of the apparatus consisted of a standard Micromerograph sample deagglomerator (Fig. 4), a 3-1/2" i.d. air sedimentation column, and a collection unit integral with a Geiger counter. The collection unit can be raised by means of a gear-and-sprocket chain drive to make a gastight seal with the column.

The collection unit itself housed a 25-3/4" diameter disc which supported 16 weighing pans, equally spaced. The pans (Fig. 5) made from 0.001-inch-thick aluminum foil, were fabricated on the forming die shown. The disc was mounted on an indexing gear driven by an eccentric drive mechanism. Indexing time was 1 second.

To minimize resuspension of the particles by convection currents, clearances were made small between the bottom of the column and the collecting pans. The apparatus was also insulated to hold the temperature variation to within ±1°C throughout the apparatus.

A Microflex timer was installed for collection at equal time intervals. For varying the time intervals, the collection disc was actuated by means of a manually operated microswitch. Cam-operated timers (Haydn) are to be installed in the future for movement of the disc at unequal time intervals.

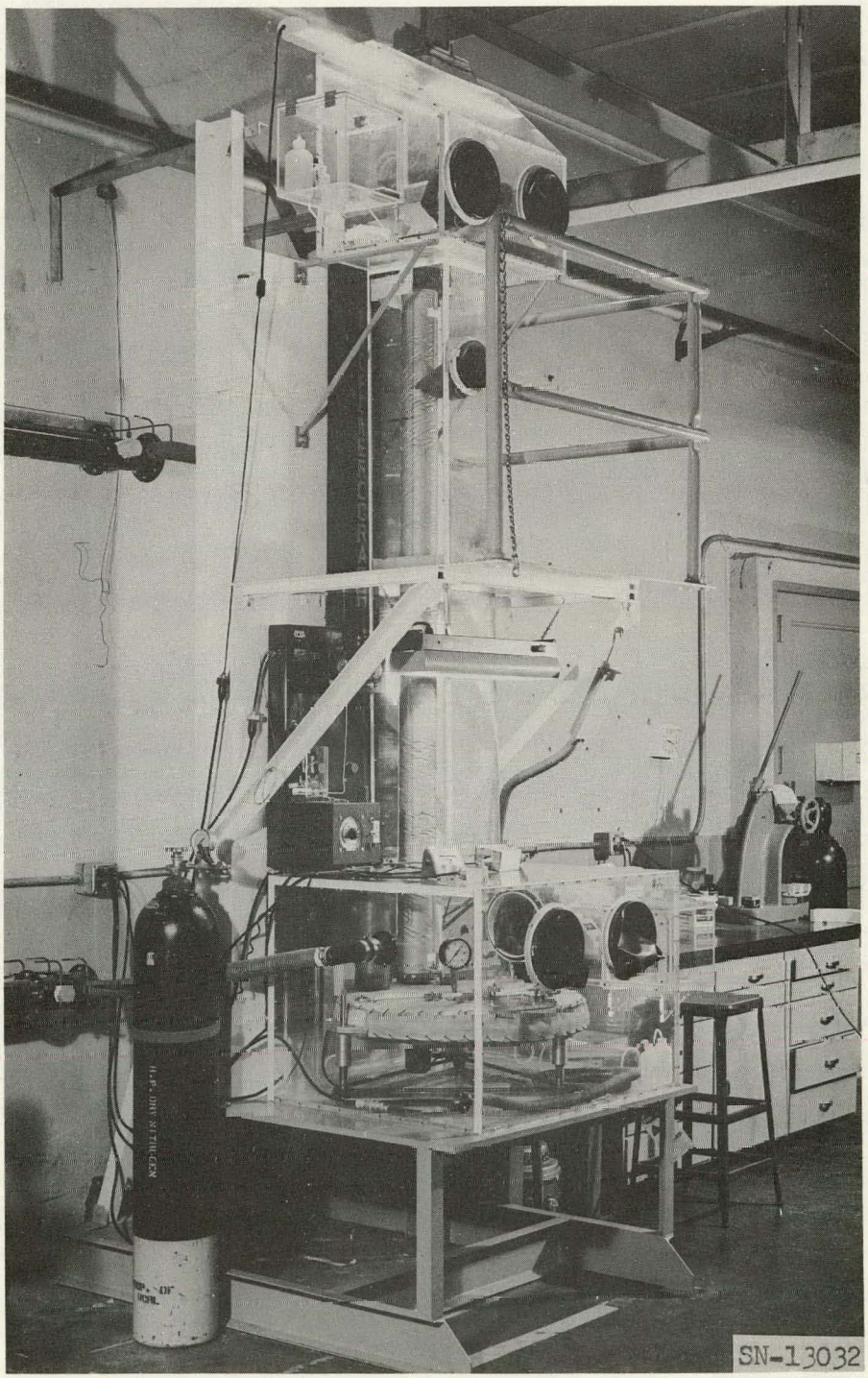

Fig. 2. General assembly of apparatus.

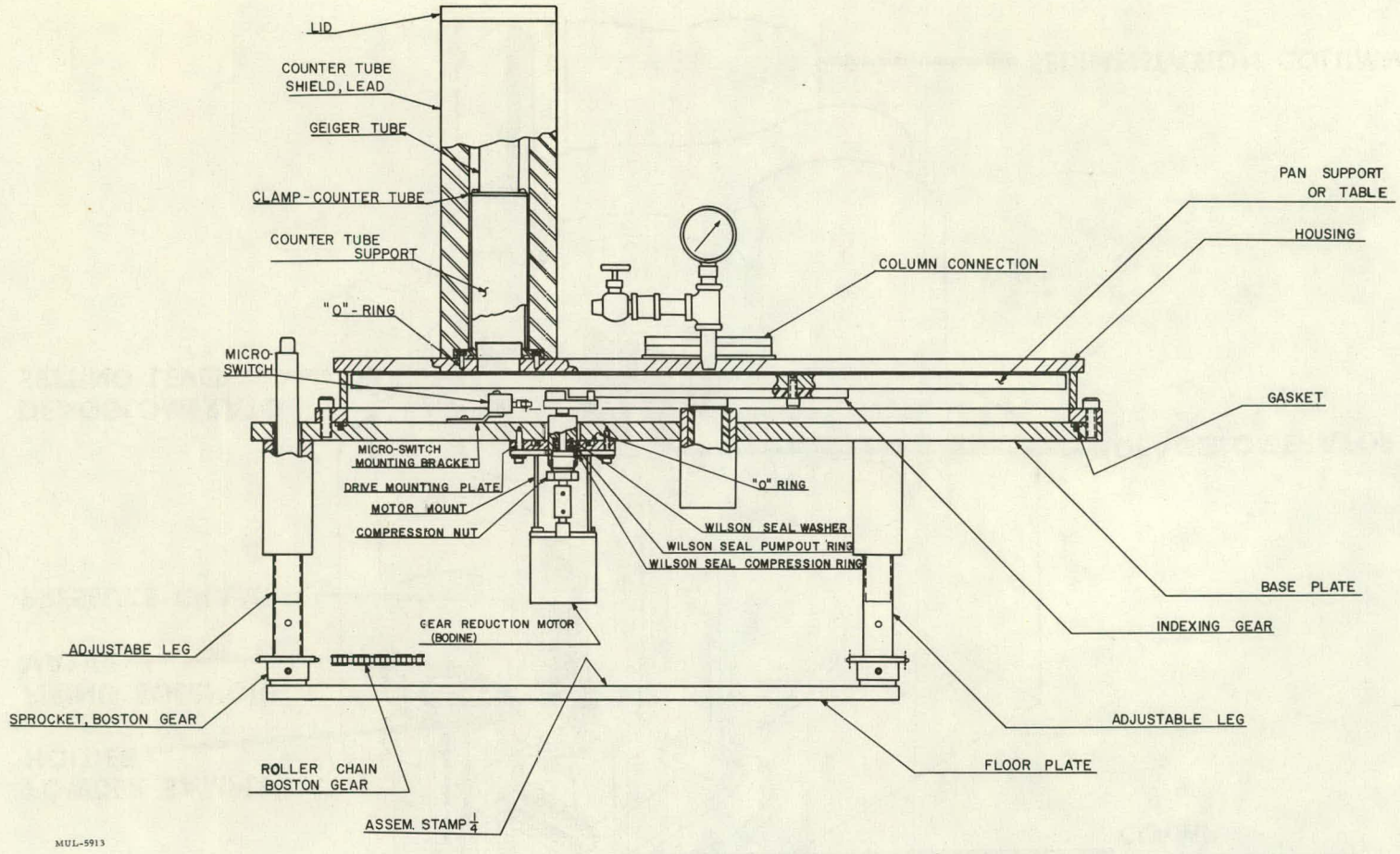

Fig. 3. Apparatus, cross section of collection mechanism.

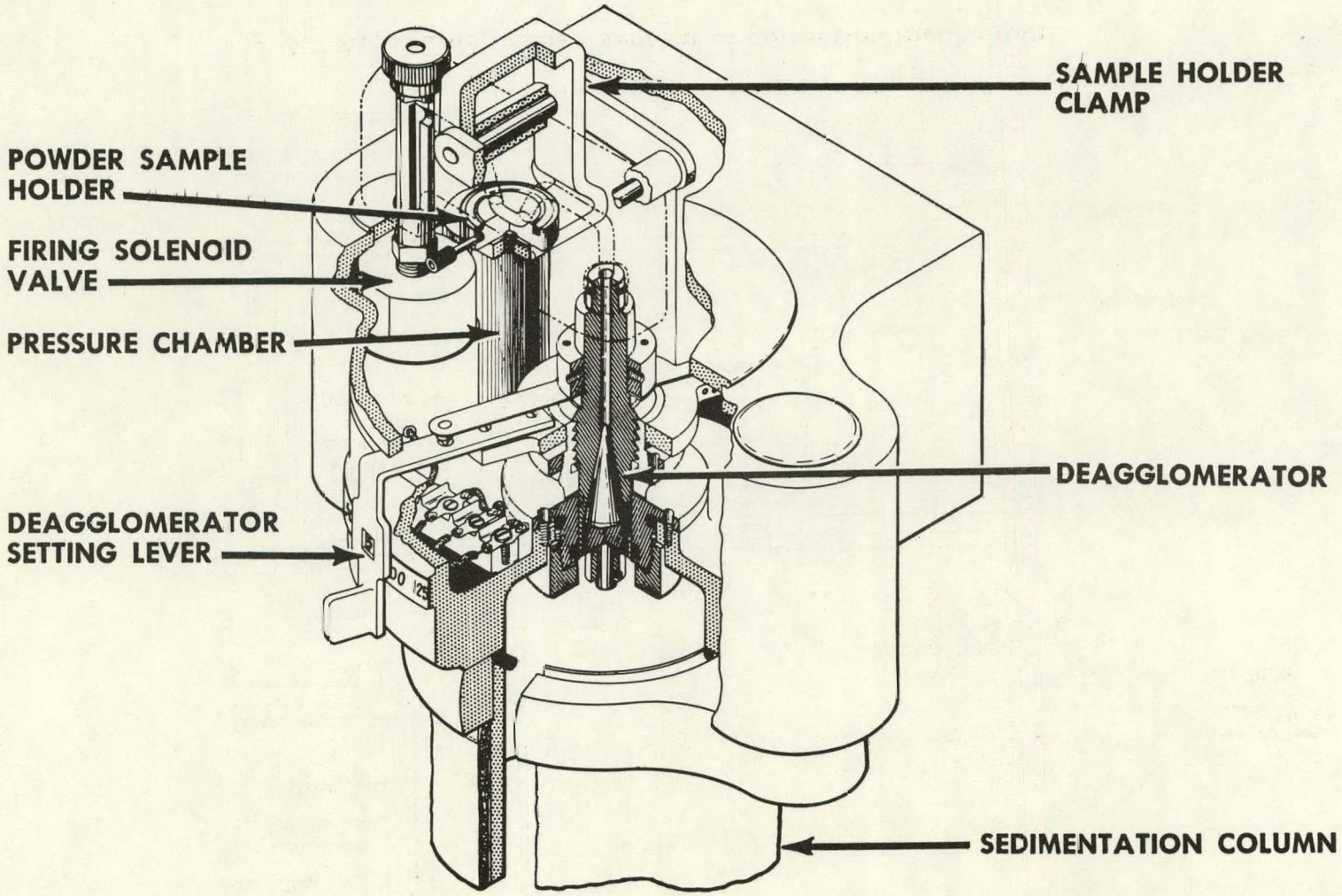

MUL-7436

Fig. 4. Section of powder sample feeder and deagglomerator.

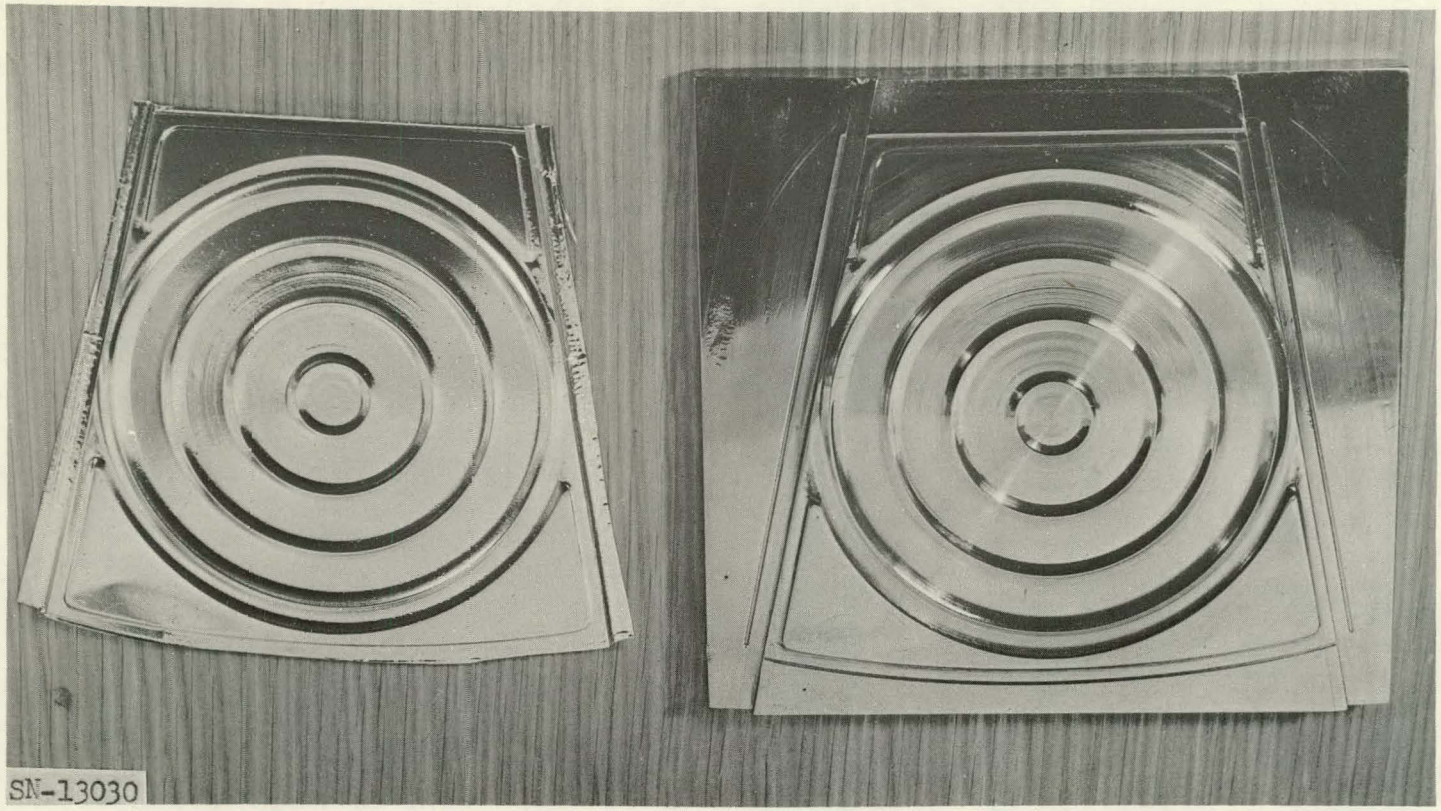

Fig. 5. Forming die and weighing pan.

The first counting of radioactivity[8] was performed with a UCRL count-rate meter (amplifier scale model L-2) and Geiger tube (Tracerlab type TGC-2). The tube was mounted over a 1-inch opening in the housing and was shielded with a 1-inch thick wall lead cylinder. In order that statistical counting would be observed, the assumption was made that a sufficient number of particles covered the foil uniformly. A source of error was encountered in some scattered radiation from adjacent samples. This scattered radiation can be largely eliminated by suitable geometrical arrangement, shielding, and electronic discrimination.

Experimental Procedure

A small pressure chamber (see Fig. 4), connected to the powder sample chamber by a solenoid valve, is charged with dry nitrogen to a predetermined pressure. When the solenoid valve is actuated, the nitrogen discharges through the powder sample and carries the powder at high velocity through a narrow slit in the deagglomerator. Powder is dispersed by the aerodynamic shear forces in the deagglomerator slit. These forces can be varied within wide limits by the choice of pressure in the pressure chamber and by the choice of the deagglomerator slit width. The former is variable from 0 to 400 psig and the latter may be adjusted from 10μ to 250μ.

The correct settings for the nitrogen feed pressure and deagglomerator slit width can be determined by making successive partial analyses with steadily increasing deagglomerating forces (higher pressures and smaller slit widths). The cumulative weight curves, as determined by weighing each pan, will move, in most cases, steadily to smaller sizes until complete deagglomeration is obtained.

Further increases in deagglomerating forces produce no changes in the particle size distribution curve until the force is great enough to break the particles. Analysis is then made of nitrogen feed pressure settings and deagglomerator slit width settings at which complete deagglomeration without breakage occurs.

DISCUSSION

In the following paragraphs are discussed some of the characteristics which apply to both the Micromeromultipan and the Micromerograph. Data obtained on the new instrument has been compared with Micromerograph data and the reproducibility of the new instrument has been treated.

A few words concerning the plotting of any particle size [9, 10, 11, 12] data is appropriate at this time. The presentation of data can be made in a variety of ways. The most commonly used methods of plotting size distribution are of the cumulative weights of material on arithmetic, log-log, log-log reciprocal, and probability scales.*

Plotting on ordinary cross section paper will produce a curve in the shape of a letter "S" (known as an ogive). Probability charts are so designed that the ogive will plot as a straight line. Hence, if the data for any series correspond exactly with the normal law of error, their ogive, plotted on the (arithmetic) probability chart, will be a straight line. Therefore, the departure of the ogive from a straight line indicates a departure from normality.

If the distribution follows the log-normal law, and we wish to obtain a straight line graph connecting particle size with frequency of occurrence, a probability grid is used whose x-axis has a logarithmic scale.

When plots are made on either probability grid, the distributions must be asymptotic at both extremes. For practical reasons, the particles measured have a smallest particle and a largest particle. Therefore, the distribution is not asymptotic. Plots on probability grid, however, often depart** from the straight line at the extremes. This would be of some concern if it were not for the fact that the areas extending from the extremes to infinity are negligible compared with the area contained under the distribution curve between the largest and smallest particles measured.

---

*Codex Book Co., Norwood, Mass.

**The cumulative percentage scale is very much expanded at each extremity. A large linear deviation in these regions parallel to the cumulative axis may not be serious. It is also believed that some departure from the straight line may be due to errors in measurement, such as selective adherence of material to the sedimentation column wall and the difficulty of measuring the time within the initial 5 seconds.

It is convenient for ground materials (e.g., the coral sample) which follow a log-normal weight distribution to adopt the method proposed by Hatch and Choate[13,14] in 1929 to describe the mathematical function of the size distribution curve* by giving values of geometric mean diameter and standard deviation.

The amount of labor involved in computing mean diameter and standard deviation is reduced by using probability grids. From such a grid, the mean and the standard deviation may be readily obtained. A horizontal line is drawn at the 50% point, (probability of 0.5) and the crossing point with the straight distribution line is projected on to the x-axis where we read the arithmetic (or log) mean particle size.

In order to obtain the standard deviation, horizontal lines are erected at the 84.13% or 15.8% points ($\pm 1\sigma$). The crossing point with the straight distribution line is projected onto the x-axis and the distance on the x axis of the projection from the mean diameter represents the standard deviation. This method will be illustrated when the reproducibility of results is discussed and the instruments compared.

Effect of Column Diameter

The question of the effect upon the velocity of fall of a particle arising from the limitation of the extent (diameter of container) of the fluid may be analyzed upon the basis of studies made by Rose, Lorentz and Faxen.[15] Their results are the following: "For particles of 50μ diameter settling in a tube of 5-cm diameter, the computed diameter of less than 10% of the particles is in error to the extent of 1% or more. For 10μ-diameter particles settling in a tube 2 cm in. diameter, the velocity of less than 2% of the number is affected to the extent of 1% or more."

For our 3-1/2 in. diameter columns, the effect of the wall upon the size distribution curve can be considered negligible.

Particle Travel Distance

Although the terminal velocities of the particles as they leave the deagglomerator are reached rapidly, the distance in which they decelerate

* E.g., $y = \frac{1}{\log \sigma_g \sqrt{2\pi}} \exp\left[-\frac{\log x - x_g}{2 \log^2 \sigma_g}\right]$

is appreciable and must be considered in determining the true fall distance. There is also some difference of particle fall distance due to different cloud lengths obtained from using different deagglomeration pressures. Figure 1 was made with spherical glass beads using a deagglomeration pressure of 100 psi. In the upper range of the Micromerograph (that is, around 100 $\rho^{0.5}$) the 50% point of a distribution would be approximately 15% smaller in diameter if 25 psi were used instead of 100, and that same point would appear to be approximately 15% larger, were 400 psi used. Pressures in between these extremes would produce somewhat smaller values of deviation. In the lower size range (that is, around 15 $\rho^{0.5}$) the deviation in micron size at the extreme pressures mentioned above was not significant at all, being of the order of 5% or less, which would mean a deviation of approximately 0.75 $\rho^{0.5}$.[16]

Upper and Lower Limits for Column

Sharples Corp.[16] has stated that at values of $D\rho^{0.5}$ greater than 240 (see Fig. 1) the actual sedimentation time is difficult to measure accurately and probably depends upon D and ρ in some combination other than $D\rho^{0.5}$. For these sizes then, different powders which have the same distribution will actually give different curves.

At sizes less than the lower limit similar arguments apply. Simple theories become appreciably inaccurate for sizes $D\rho^{0.5}$ less than 2. The powder can be weighed, however, if the experiment is run long enough in order to give an accurate percentage by weight of sizes less than $D\rho^{0.5}$.

Deagglomeration Pressures

Figures 6 and 7 illustrate the results obtained in determining the proper deagglomeration pressures for coral and radiological fallout respectively. The curves for coral show a definite shift to finer particle sizes with increasing pressures. The curves for fallout do not. The proper deagglomeration pressure* for coral would be 200 psi and for fallout,

*If, with increasing pressure, a range of pressures is observed over which no shift in the particle size distributions toward the smaller particle sizes occurs, then a feed pressure in this range should be chosen for subsequent analyses. In this range the large particles do not break as they may at higher pressures and also do not remain agglomerated as may frequently occur at lower pressures. Commonly, all curves will lie on top of one another above some minimum pressure. In many such cases particle breakage does not take place within the range of feed pressures provided, and degglomeration is good at all pressures above the minimum. See also Sharples Manual for further discussion.

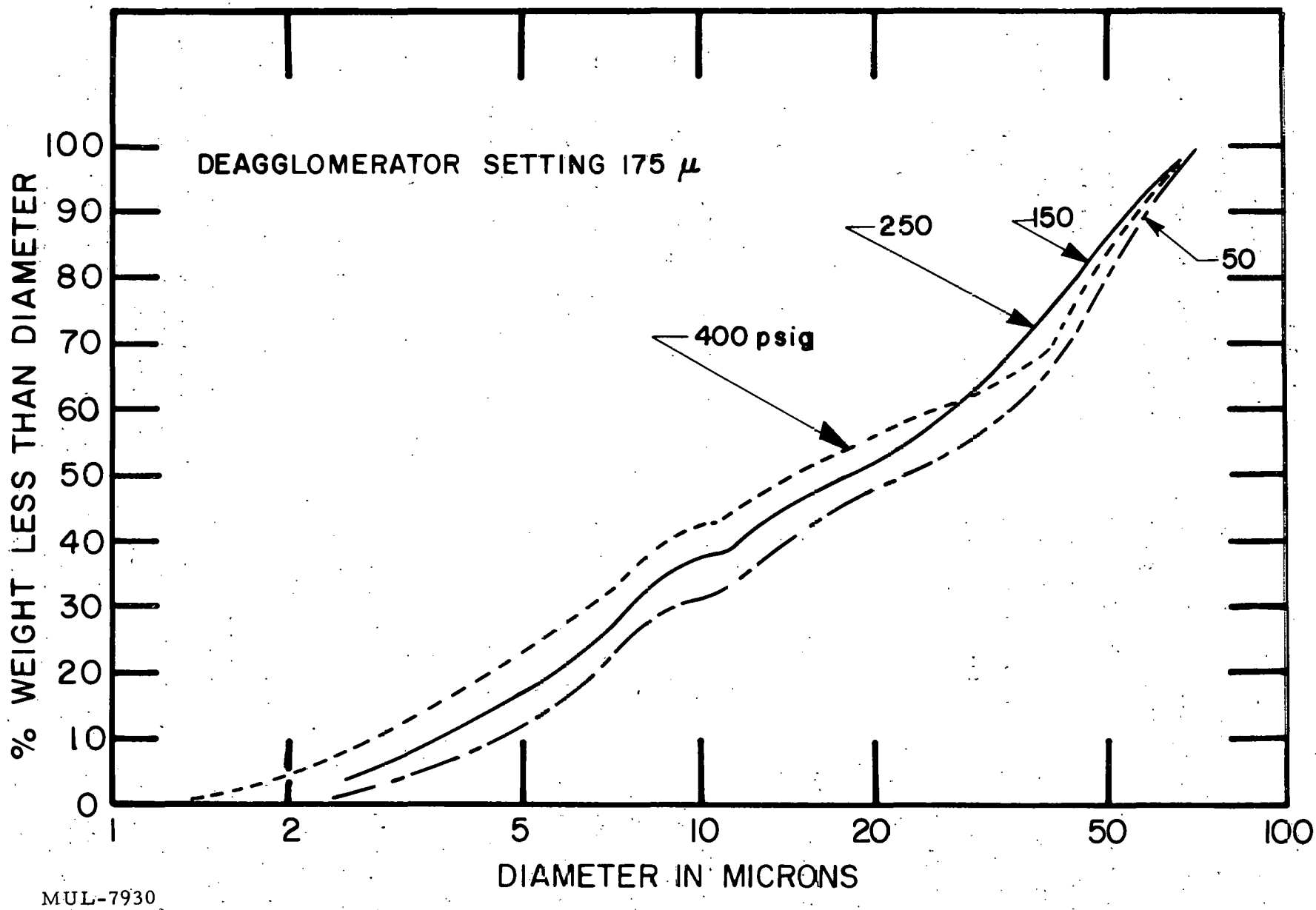

Fig. 5. Distribution curves from trial pressure runs, coral sample.

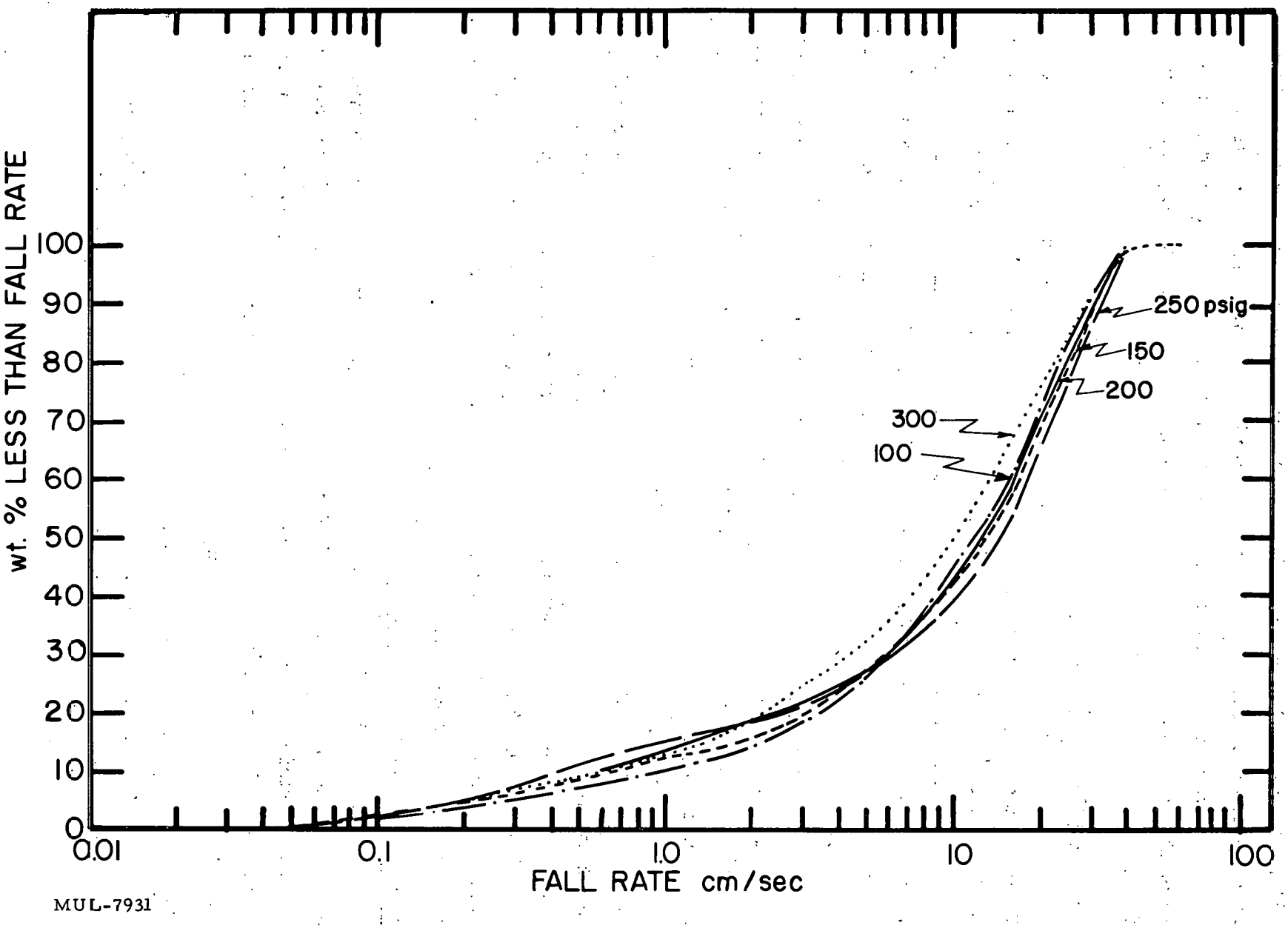

Fig. 7. Distribution curves from trial pressure runs, fallout sample.

100 to 200 psi. The pattern for fallout samples is not so well defined and much judgment must be used in determining the "proper" pressure.

If one selects pressures wisely, there is no further need to make runs at e.g., 300 and 400 psi. This is illustrated in Fig. 12, the curve for a Pb powder.

Deagglomerator Slit Widths

A deagglomerator setting of 250μ will nearly always be satisfactory. There are occasions when an opening twice the diameter (2·D) of the largest particle expected may be required for sufficient deagglomeration.

In order to compare a 250μ with a 2·D slit width, a coral sample ($\rho = 2.8$, particle range 2μ - 90μ) was classified into four fractions. A Micromerograph particle analysis on each fraction was made using the 250μ and 2·D slit openings.

Figures 8, 9, 10, and 11 illustrate the results obtained. To the right of the 10μ diameter, the curves for the two settings coincide, or very nearly coincide. To the left of this particle diameter, the size distribution curves are shifted to finer particle sizes by using a 250μ opening.

In analyzing the discrepancies in the analyses obtained with openings of 250μ and 2·D, it appears as though the 2·D openings caused some turbulence at the top of the column and a somewhat selective holdup of the finer material. The error is not serious in this case because a composite curve calculated from the fractions agrees very well with the curve from the unfractionated sample. Fraction 18F in the above figures amounted to only 2.7% of the original sample.

Weight of Sample Charged

Figure 13 represents a size distribution curve for a composite sample of coral using 30- and 100-mg samples, and Figure 14 represents the size distribution curve for the coarsest fraction using 30- and 100-mg samples. There is no appreciable difference in the curves for either the 30-mg samples or 100-mg samples.

Comparison with Micromerograph

The question arises whether the results, Figs. 15 and 16, reached by the Micromeromultipan and Micromerograph can be regarded as being

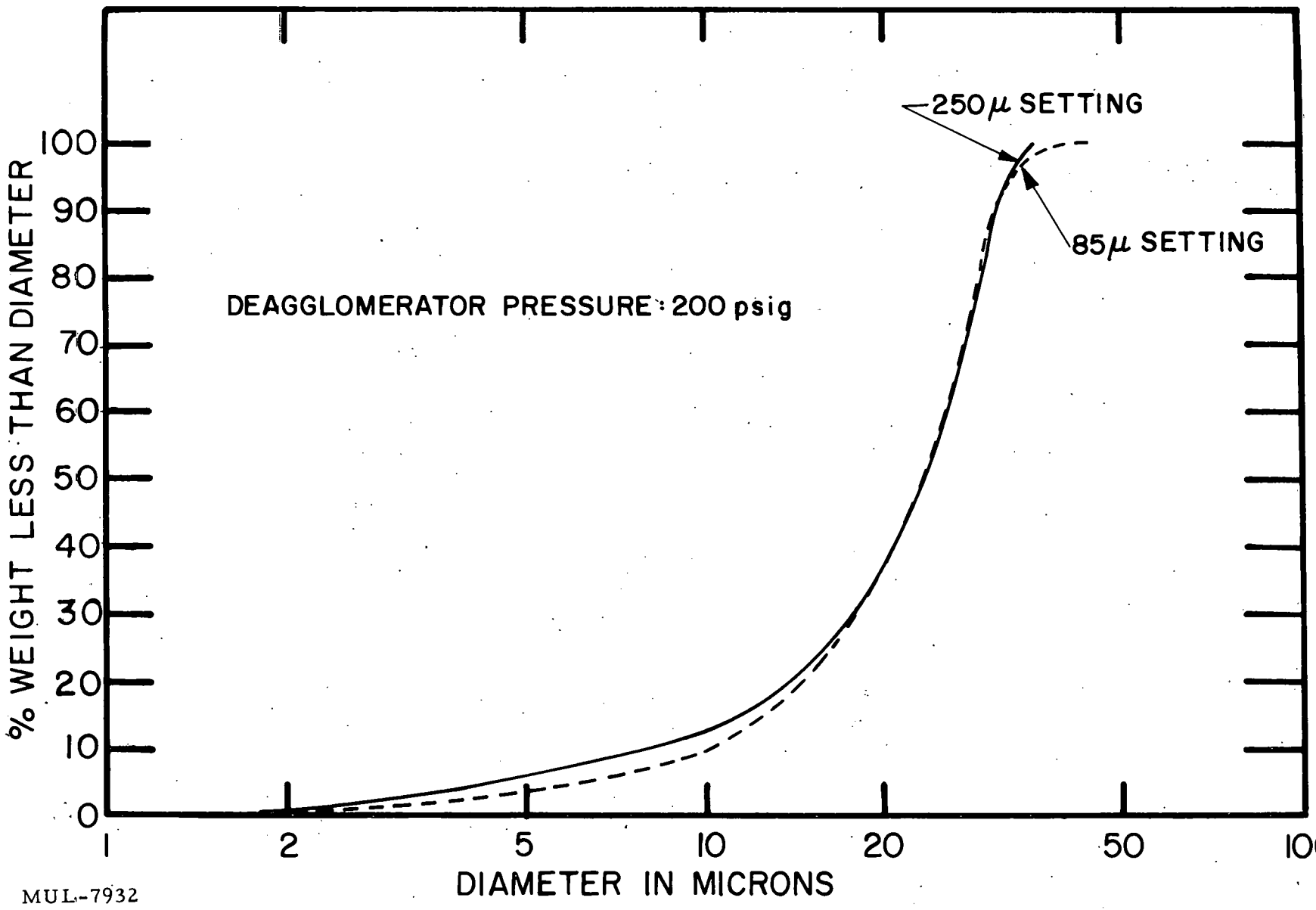

Fig. 8. Particle size distribution analysis curves for 85μ and 250μ slit width for a sample of fractionated coral, 4F. Order of fineness of sample: 4F (coarsest), 12F, 16F, 18F (finest).

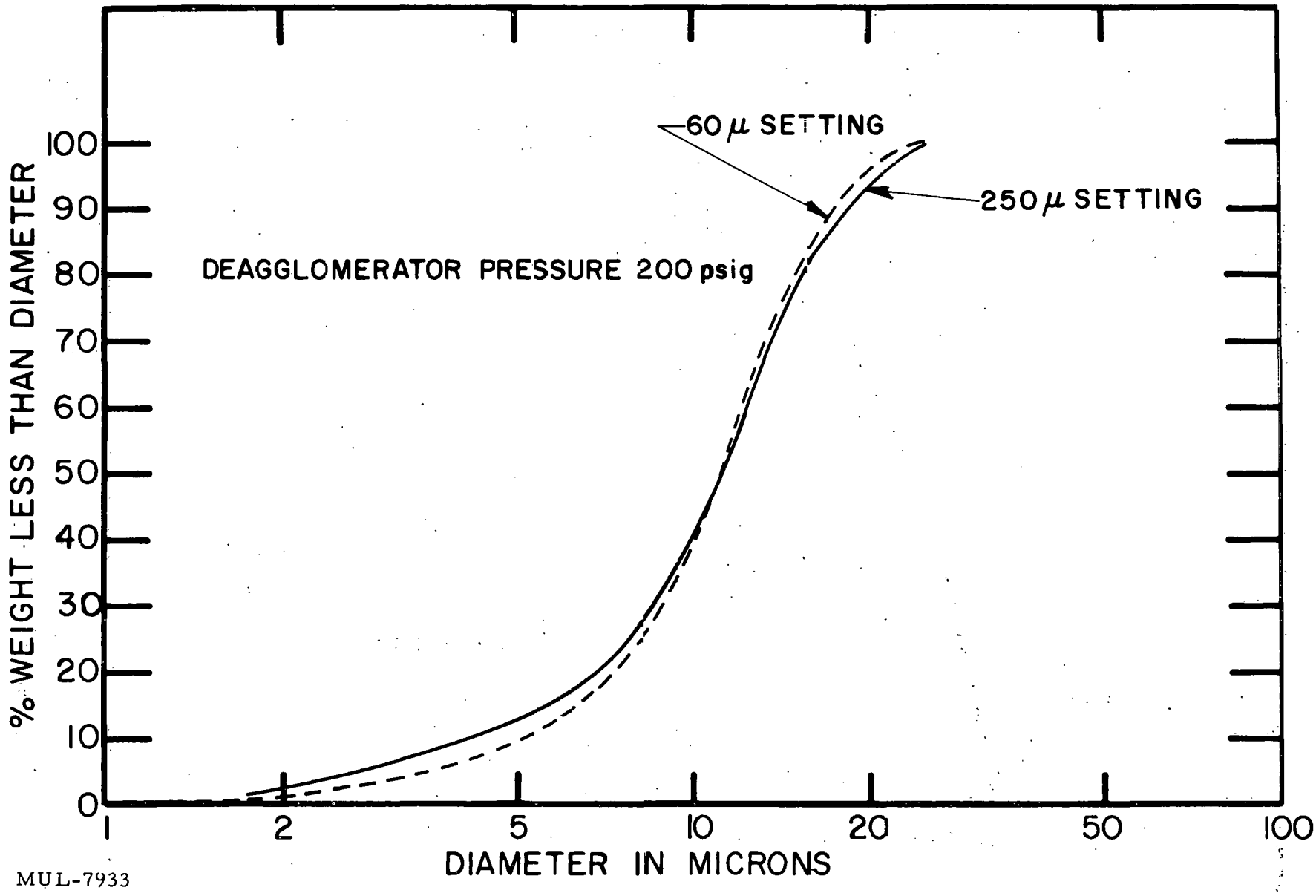

Fig. 9. Particle size distribution analysis curves for 60μ and 250μ slit width for a sample of fractionated coral 12F. Order of fineness of sample: 4F (coarsest), 12F, 16F, 18F (finest).

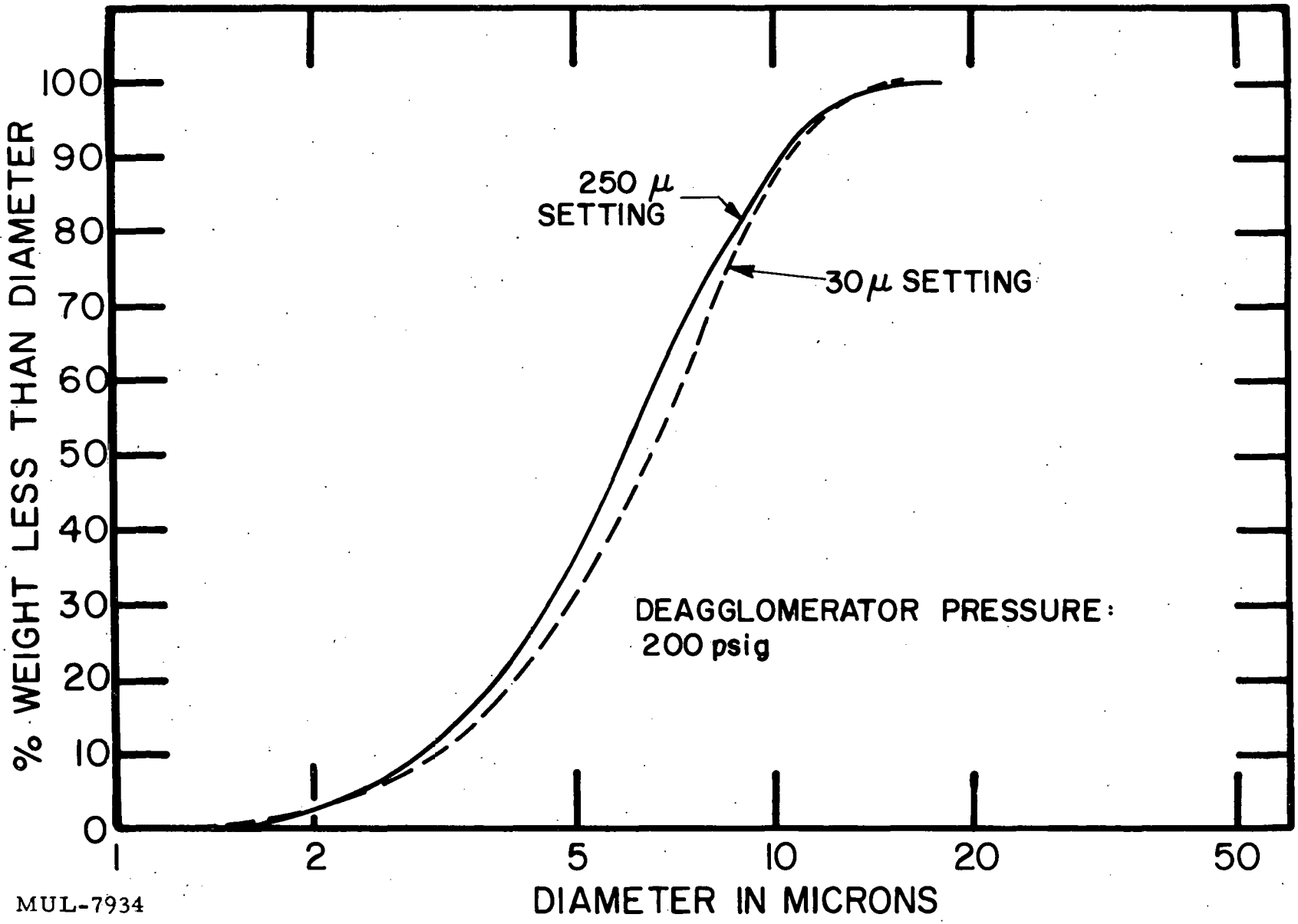

Fig. 10. Particle size distribution analysis curves for 30μ and 250μ slit width for a sample of fractionated coral, 16F. Order of fineness of sample: 4F (coarsest), 12F, 16F, 18F (finest).

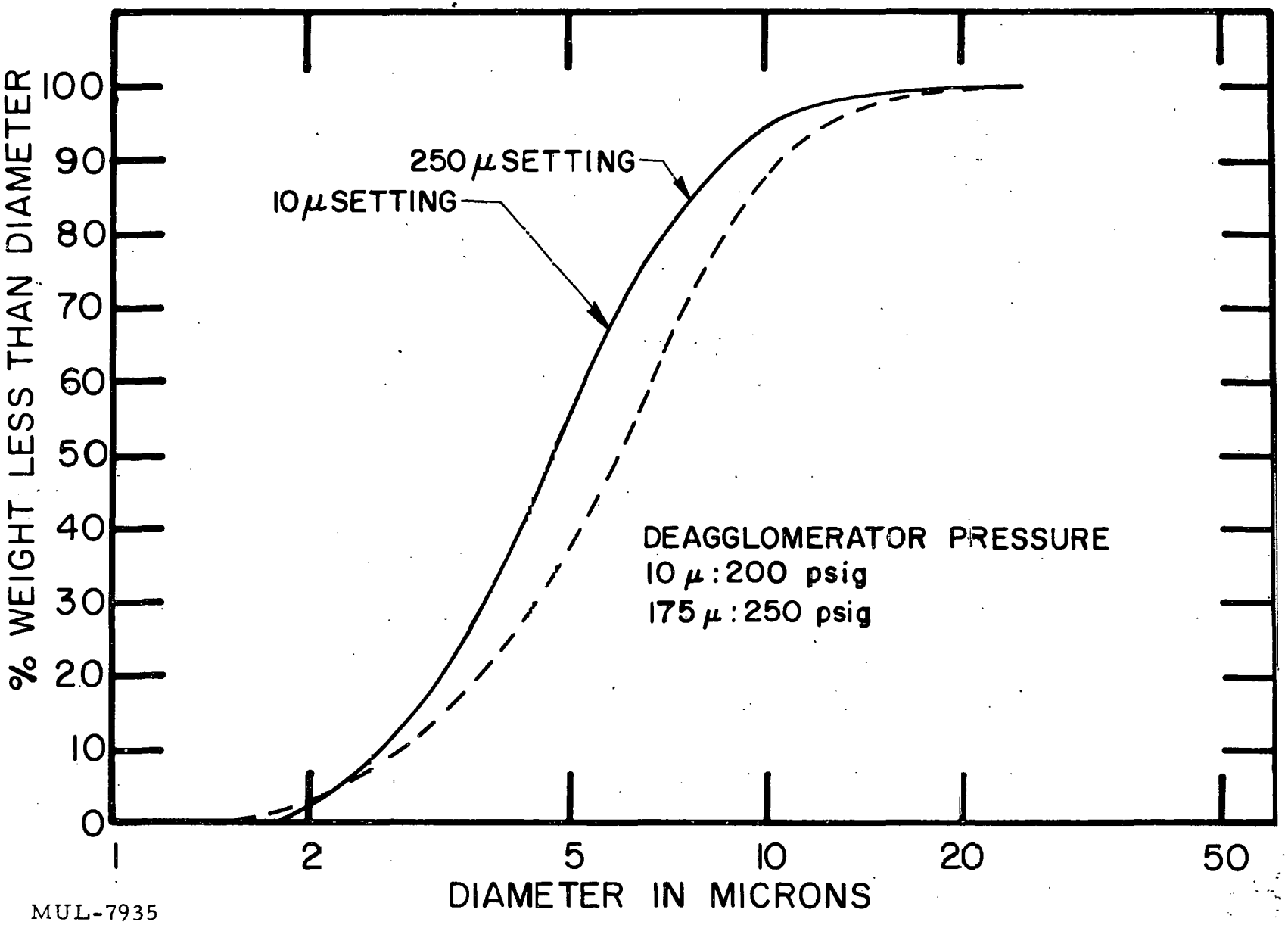

Fig. 11. Particle size distribution analysis curves for 10μ and 250μ slit width for a sample of fractionated coral, 18F. Order of fineness of sample: 4F (coarsest), 12F, 16F, 18F (finest).

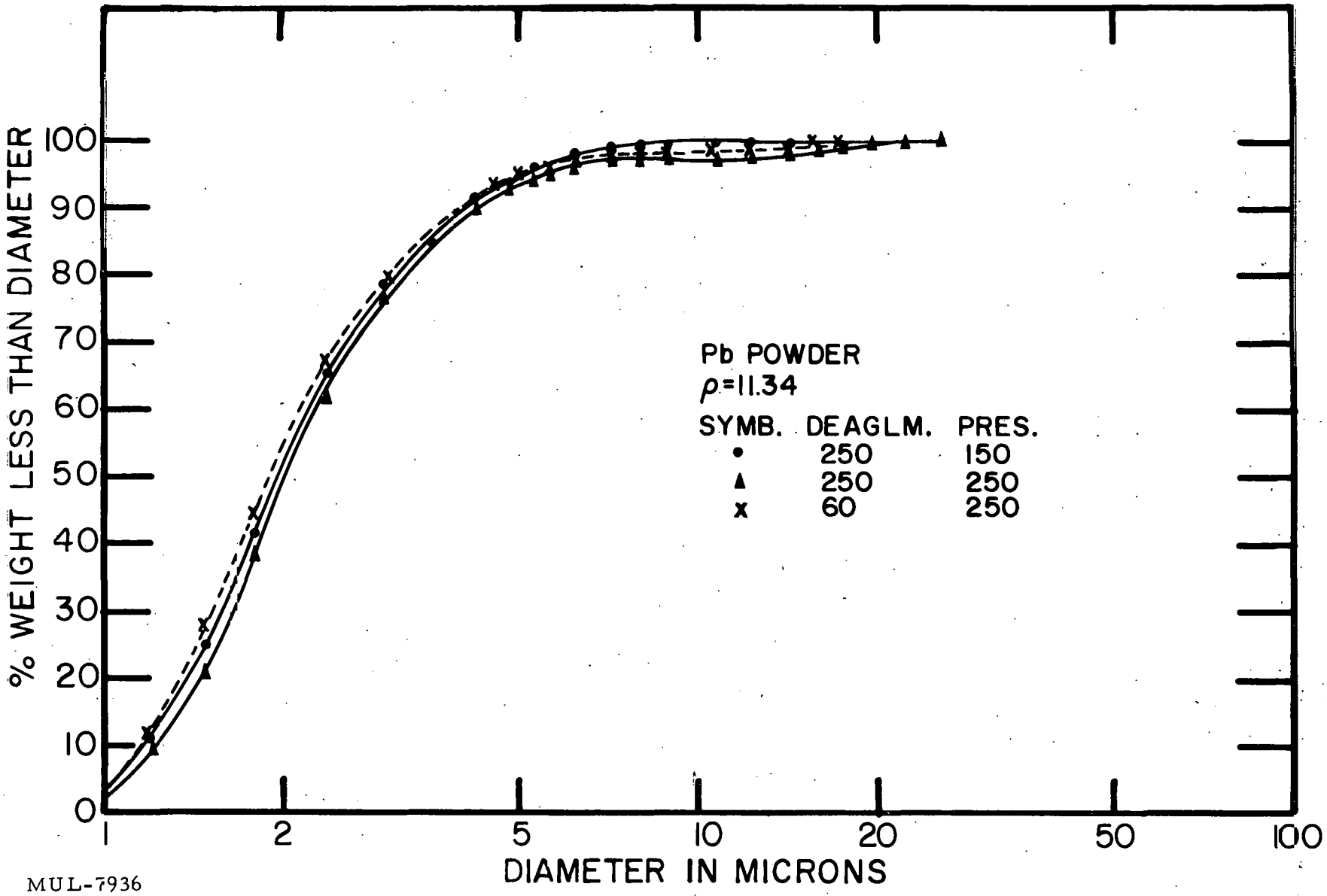

Fig. 12. Distribution curves for a Pb powder.

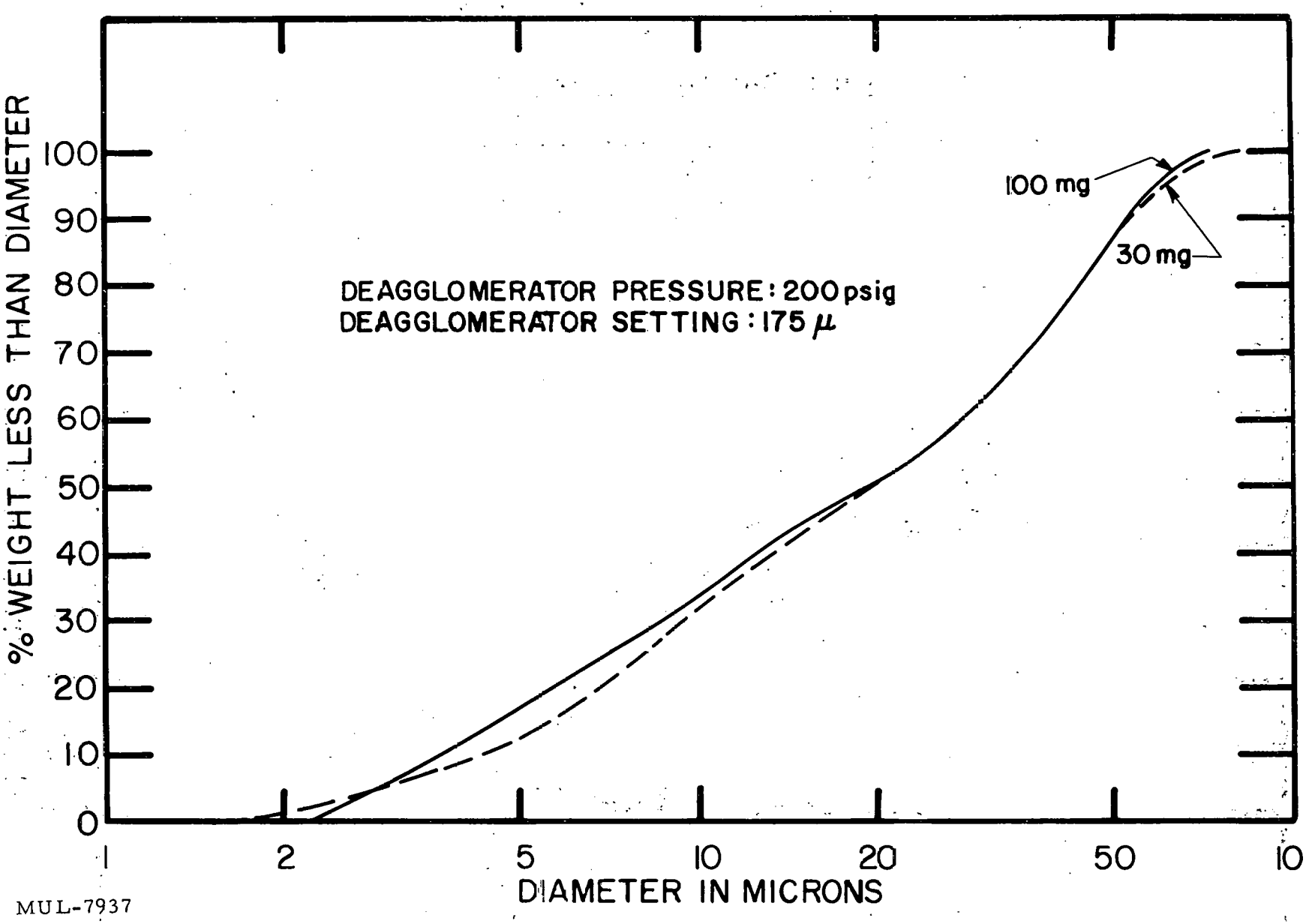

Fig. 13. Particle size distribution analysis curves for coral, 30 mg and 100 mg samples.

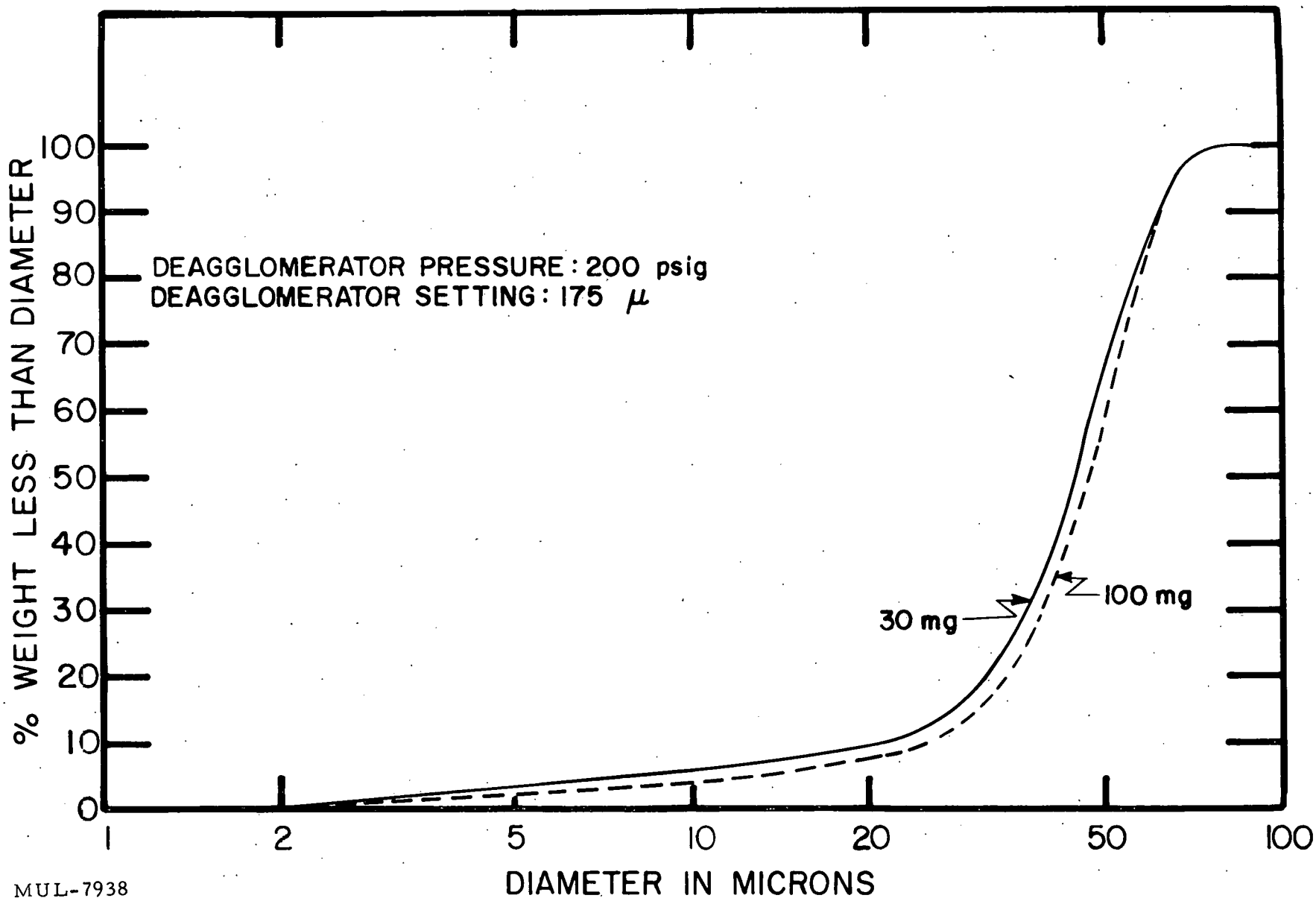

Fig. 14. Particle size distribution analysis curves for a coarse fraction of coral using 30 mg and 100 mg samples.

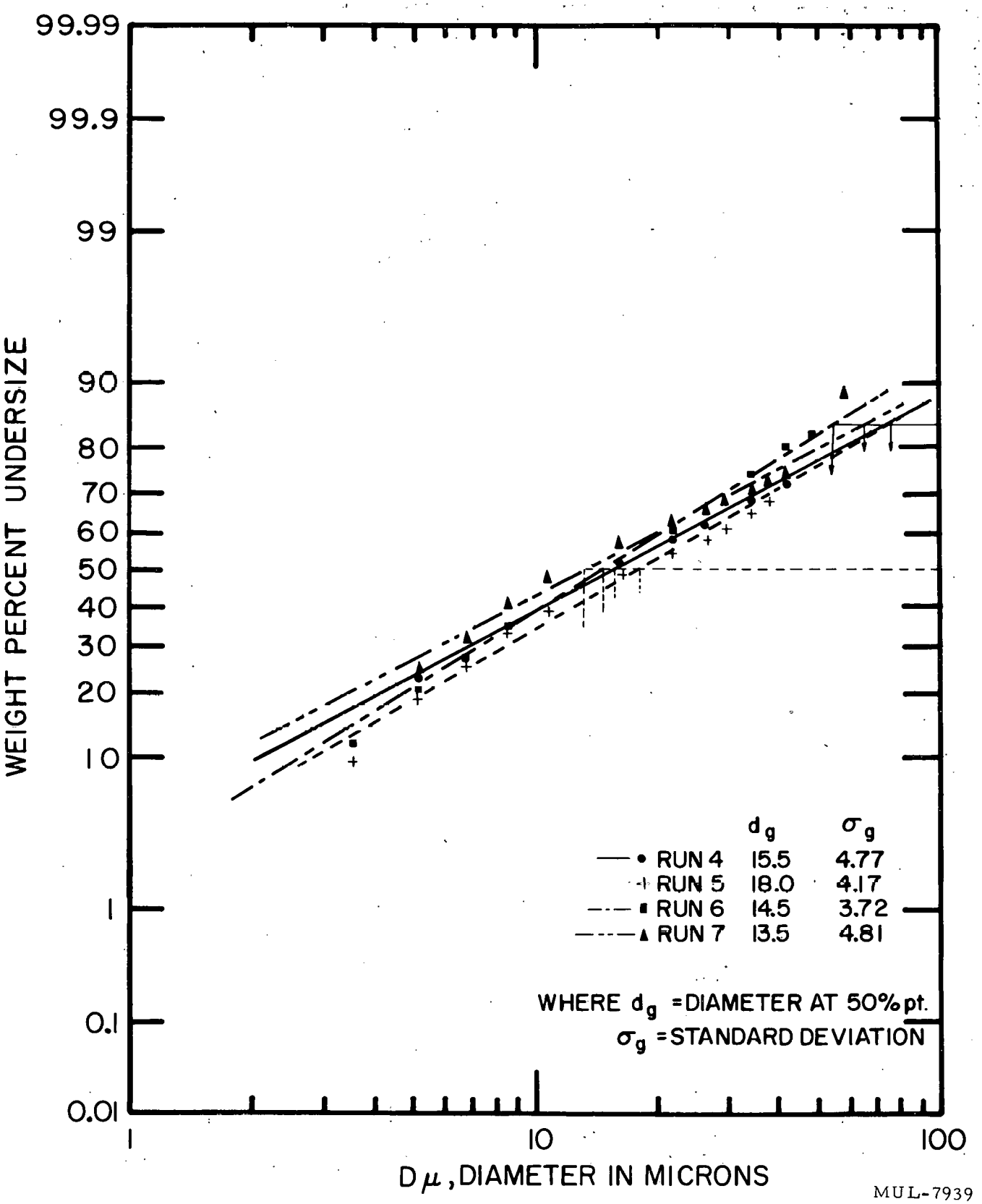

Fig. 15. Distribution curve for coral, Micromeromultipan analysis.

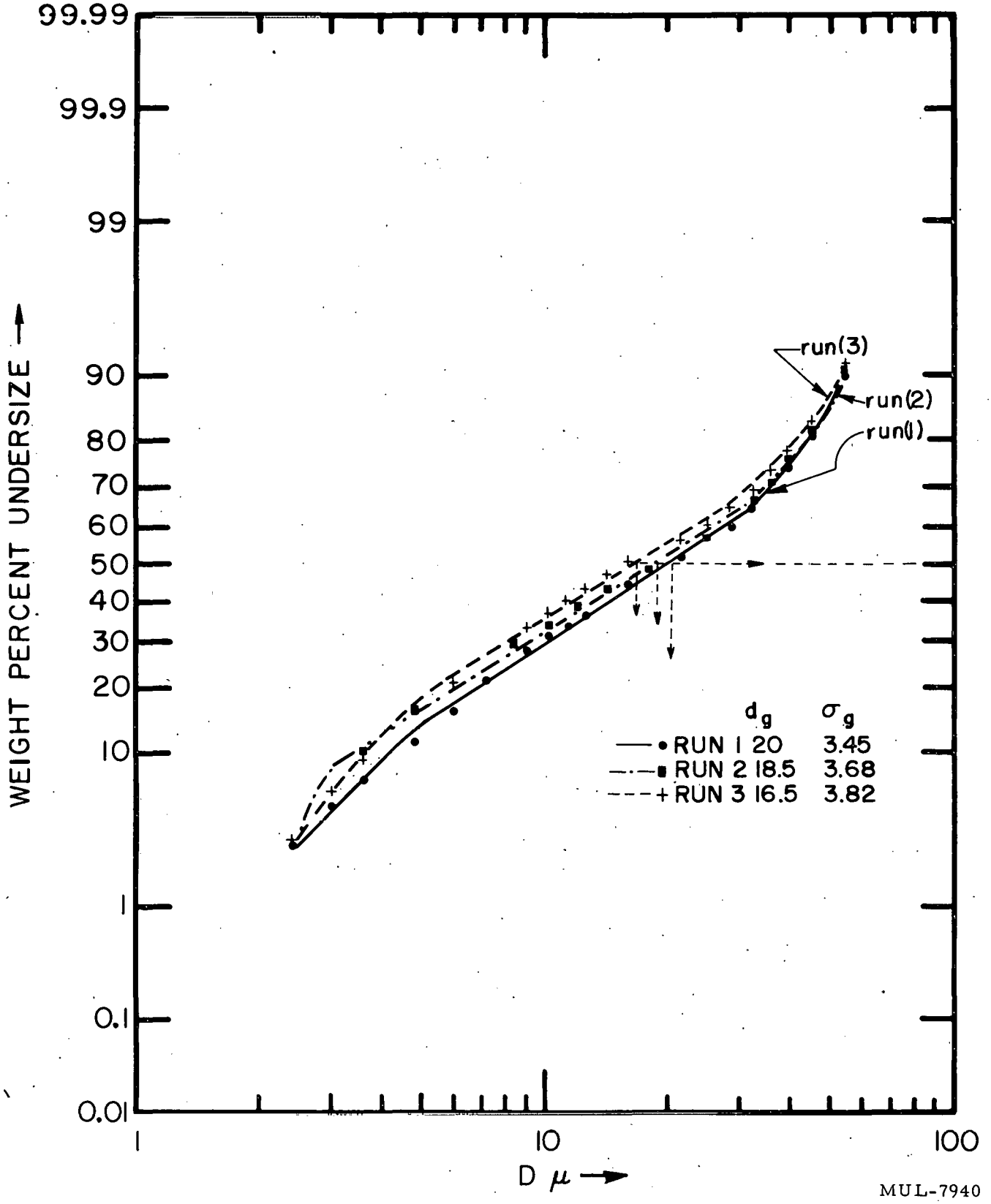

Fig. 16. Distribution curve for coral, Micromerograph analysis.

reasonably the same or whether the difference in the method of determination leads to a real difference between the results. For this we apply the "t-test."[17]

The following percentages of particles by weight, smaller than 15 microns, were obtained for each instrument.

	Micromeromultipan		Micromerograph	
	X_1 (in %)	X_1^2	X_2 (in %)	X_2^2
	53	2,809.00	47	2,209.00
	51	2,601.00	44	1,936.00
	49	2,401.00	41	1,681.00
	45	2,025.00		
Totals:	198	9,836.00	132	5,826.00

The quantities to be calculated for the "t-test" are:

$$\bar{x}_1 = 49.5 \qquad \bar{x}_2 = 44$$

$$\Sigma x_1^2 = 9,836 \qquad \Sigma x_2^2 = 5,826$$

$$n_1 \bar{x}_1^2 = 4(2450.25) = 9801 \qquad n_2 \bar{x}_2^2 = 3(1936) = 5808$$

$$\sigma\Delta = \sqrt{\frac{(\Sigma x_1^2 - n_1 \bar{x}_1^2) + (\Sigma x_2^2 - n_2 \bar{x}_2^2)}{n_1 + n_2 - 2}} \cdot \sqrt{\frac{n_1 + n_2}{n_1 \cdot n_2}}$$

$$= \sqrt{\frac{35 + 18}{5}} \cdot \sqrt{\frac{7}{12}} = 2.485$$

$$t = \Delta/\sigma_\Delta = 5.5/2.49 = 2.21$$

where σ_Δ is the standard deviation, n is the number of samples, $\bar{x}$ is the mean of the sample, and $\bar{x}_1 - \bar{x}_2 = \Delta$, the difference between the means which for 5 degrees of freedom $(n_1 + n_2 - 2)$ is not significant at the conventional level, i.e., at the 0.05 of t. We can conclude that the two instruments lead to reasonably the same result.

Figure 17 represents a standard "S" plot of a fallout sample (run in duplicate) collected in 1955 which was analyzed on the Micromeromultipan. The two curves are in good agreement with each other.

Reproducibility of Results[18]

A convenient measure of reproducibility or precision is the reciprocal of the standard deviation or the reciprocal of its square. For the purpose of comparing two runs, the difference or ratio of their standard deviations must be tested for significance.

Taking, for instance, the standard deviation of runs 4 and 6, Fig. 15, we get 4.77 and 3.72 respectively. Taking the ratio of squared deviations of these two quantities, the numerator being the larger of the two quantities, we find from a table for the variance ratio or F-function that the difference between the reproducibility of results in runs 4 and 6 is not significant at the 5% level of probability.

Recovery of Sample

Micromeromultipan vs Micromerograph. Fallout samples run on the Micromeromultipan gave an average recovery of 45% as compared to 51% recovery on the Micromerograph. In the work with coral samples, 56% was recovered on the Micromeromultipan as against 65% on the Micromerograph. The lower values for the Micromeromultipan are believed to be due to the fact that drier air had been used in the column, resulting in more static charge.

Dependence of Distribution Curve Upon Percent Recovery. The size distribution curve is independent of the recovery for a particular sample. Figure 17 demonstrates this fact well. Run No. 1 produced 33.7% and run No. 2 gave 48.4% for the recovery of the sample. Apparently the holdup is not selective in this range. The reason for differences in recovery has not been satisfactorily explained, but it may be due to differences in surface charges in the apparatus. This charge can be reduced by the use of anti-static agents (Anstac).

Recovery and Accuracy of Results. A few words may be said concerning recovery and accuracy of the results. If all the material charged to the instrument were recovered on the pans, there would be little doubt

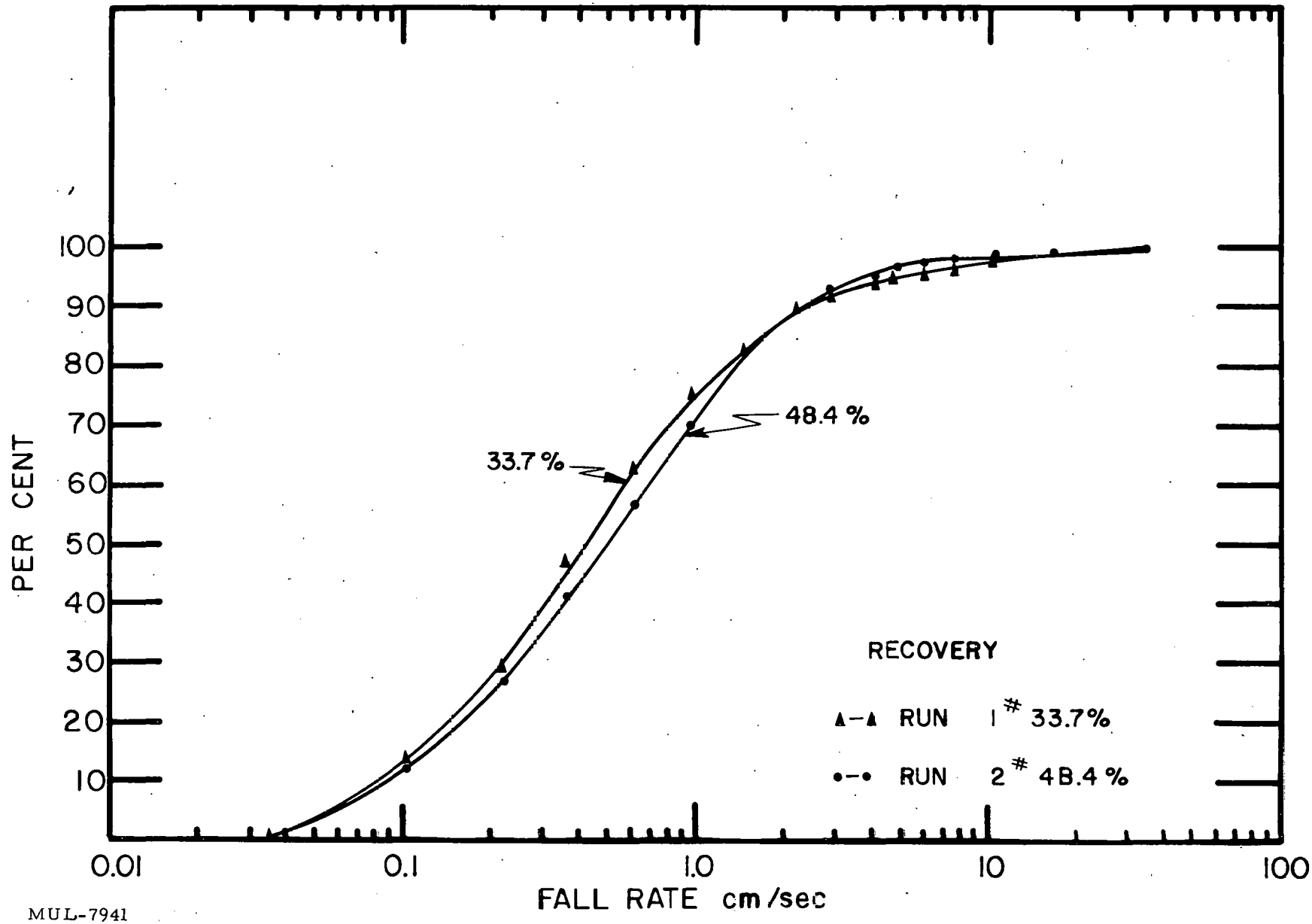

Fig. 17. Distribution curves for fallout, Micromeromultipan analysis.

about the accuracy of the analysis. There is also another area of concern when the recovery of the sample is low and the particle sizes are very small. It is this: Are the finer particles lost to the wall by impingement and electrostatic action in preference to the larger ones (classification), or is the loss equally distributed among all the particles. If the loss is distributed equally, then we can say that the size distribution curve is the same in the fraction lost as in the sample fraction recovered.

There is another problem with reference to the fallout samples themselves. If we assume that the "particles" can be a sintered agglomerate of perhaps 2, 3 or 4 discrete particles and that they are not broken up by the sample collecting mechanism (impact on filter, etc.) then we can say that we start with a true sample being fed to the air sedimentation apparatus. If we assume that the "particles" have lasted this long, then we again have to determine whether the sintered bond between each discrete particle is either stronger or equal to the strength of the fallout material itself in order that the bond is not disturbed in the deagglomerator of the sedimentation apparatus.

Only, if at some future date, we can obtain fallout samples as they exist in the atmosphere, will we be able to obtain a truer picture of the situation.

CONCLUSIONS

A standard Micromerograph Unit was adapted to fractionate a column of settling fallout particles. Each particle grouping could be weighed and then counted for radioactivity by means of a Geiger tube placed directly over the fractionating pan or each pan could be removed and counted for activity in a separate counting chamber.

Several characteristics of the unit have been discussed. There is no effect of a 3-1/2-inch column on the settling velocity of the particles. The column height is sufficient to accommodate deceleration of the particle. Limits have been placed on the column using $D\rho^{0.5} = 240$ as the upper limit and $D\rho^{0.5} = 2$ as the lower limit. Further evaluation has shown that the sample sizes between 30 and 125 mg have no effect on the distribution curve. The deagglomerator slit width of 250μ is preferable.

The "t" test (statistical) has shown that the differences between the Micromeromultipan and the Micromerograph are not significant. Using the statistical F-function tables, it has been shown that the Micromeromultipan reproduces data well.

ACKNOWLEDGMENT

Thanks are due to D. Hanner and R. Heminger for their help in collecting the particle size data.

References

1. J.H. Perry, Chemical Engineers Handbook, McGraw Hill Book Co., Inc., N.Y., 1950.
2. R.D. Cadle, "Particle Size Determination," Interscience Publishers, Inc., N.Y., 1955.
3. L.T. Work and K.T. Whitby, "Size Measurement of Particles," Encyclopedia of Chemical Technology, 12 Interscience Encyclopedia Inc., 1954.
4. B.M. Abraham, H.E. Flotow and R.D. Carlson, "Particle Size Determination by Radioactivation," Analytical Chemistry, 29, 1058 (11 1957).
5. G.W. Leddicotte, H.R. Miller, R.E. Druschel, M.T. Kelley, and L.C. Bate, "Particle Size Distribution Analysis of Radioactive Materials," ORNL rough draft of report to Bendix Corp., Kansas City, Mo. (1958).
6. C.N. Davies, "Symposium on Particle Size Analysis," The Institution of Chemical Engineers (London) 25-39 (Feb. 4, 1947).
7. H.E. Rose, "The Measurement of Particle Size in Very Fine Powders," Constable and Co., Ltd., London, 1954, p. 41.
8. W.R. Jordan, Annual Rev. of Nuclear Science, 1 209 (1952) Annual Reviews, Inc., Stanford, Calif.
9. J.B. Austin, "Methods of Representing Distribution of Particle Size." I.E.C., Anal. Ed. VII, 334-9 (JE 1939).
10. C.E. Lapple, "Mist & Dust Collection," Heating, Piping and Air Conditioning 18, 108-113 (1946).
11. J.M. Dalla Valle, "Micromeretics," Pitman Publishing Corp., N.Y., pp. 55-7.
12. G. Herdan, "Small Particle Statistics," Elsevier Publishing Co., N.Y., pp. 125-42
13. T. Hatch and S.P. Choate, "Statistical Description of the Size Properties of Non-Uniform Particulate Substances." J. Franklin Inst. 207 369 (1929).
14. T. Hatch, ibid. 215 27 (1933).
15. H.E. Rose, op. cit. p. 42.
16. Sharples Corp., private communication.
17. G. Herdan, op. cit. p. 143-195.
18. G. Herdan, op. cit. p. 143-195.